The Cryosphere, 8, 705–720, 2014
www.the-cryosphere.net/8/705/2014/
doi:10.5194/tc-8-705-2014

The Cryosphere Open Access

Uncertainties in Arctic sea ice thickness and volume: new estimates and implications for trends

M. Zygmuntowska[1,2], P. Rampal[1], N. Ivanova[1], and L. H. Smedsrud[2]

[1]Nansen Environmental and Remote Sensing Center, Bergen, Norway
[2]Geophysical Institute, University of Bergen, Bergen, Norway

Correspondence to: M. Zygmuntowska (marta.zygmuntowska@nersc.no)

Received: 4 September 2013 – Published in The Cryosphere Discuss.: 11 October 2013
Revised: 20 February 2014 – Accepted: 3 March 2014 – Published: 22 April 2014

Abstract. Sea ice volume has decreased in the last decades, evoked by changes in sea ice area and thickness. Estimates of sea ice area and thickness rely on a number of geophysical parameters which introduce large uncertainties. To quantify these uncertainties we use freeboard retrievals from ICESat and investigate different assumptions about snow depth, sea ice density and area. We find that uncertainties in ice area are of minor importance for the estimates of sea ice volume during the cold season in the Arctic basin. The choice of mean ice density used when converting sea ice freeboard into thickness mainly influences the resulting mean sea ice thickness, while snow depth on top of the ice is the main driver for the year-to-year variability, particularly in late winter. The absolute uncertainty in the mean sea ice thickness is 0.28 m in February/March and 0.21 m in October/November. The uncertainty in snow depth contributes up to 70 % of the total uncertainty and the ice density 30–35 %, with higher values in October/November. We find large uncertainties in the total sea ice volume and trend. The mean total sea ice volume is $10\,120 \pm 1280\,\mathrm{km}^3$ in October/November and $13\,250 \pm 1860\,\mathrm{km}^3$ in February/March for the time period 2005–2007. Based on these uncertainties we obtain trends in sea ice volume of $-1450 \pm 530\,\mathrm{km}^3\,\mathrm{a}^{-1}$ in October/November and $-880 \pm 260\,\mathrm{km}^3\,\mathrm{a}^{-1}$ in February/March over the ICESat period (2003–2008). Our results indicate that, taking into account the uncertainties, the decline in sea ice volume in the Arctic between the ICESat (2003–2008) and CryoSat-2 (2010–2012) periods may have been less dramatic than reported in previous studies. However, more work and validation is required to quantify these changes and analyse possible unresolved biases in the freeboard retrievals.

1 Introduction

Remotely sensed estimates of sea ice area and thickness reveal a dramatic decline in Arctic sea ice volume in the last decades (Kwok et al., 2009; Laxon et al., 2013). This decline mirrors changes in the Arctic heat budget (e.g. Kurtz et al., 2011b; Perovich et al., 2011) and alters the exchange of freshwater between sea ice and the ocean (e.g. Aagaard and Carmack, 1989; McPhee et al., 2009). As they are of primary importance for the Arctic (Screen and Simmonds, 2010) and the global climate system (Outten and Esau, 2012), these remotely sensed data have been analysed in many studies. Unfortunately, many of the studies lack a detailed estimate of uncertainties. We fill this gap and quantify total uncertainties in sea ice thickness and volume in the Arctic basin. We further identify the main factors contributing to the uncertainties, analysing snow depth, sea ice density and area. We provide uncertainties averaged over the Arctic basin and analyse the spatial and seasonal variability.

Arctic sea ice area has been observed from satellites over the last 40 yr starting with the Nimbus 5 electrically scanning microwave radiometer (ESMR) in 1972. A decrease in sea ice area was detected in the early 1990s (Serreze et al., 1995; Parkinson et al., 1999) and has continued at an increased rate in the last decade (Cavalieri and Parkinson, 2012). The average difference in daily sea ice extent among the most known algorithms can reach up to ± 1 million km^2, but it seems difficult to get a grip on which algorithm produces the most correct estimates.

Until the 1990s, our knowledge of Arctic sea ice thickness was determined by sparse field campaigns or submarine measurements giving only limited insight into the overall Arctic sea ice thickness. Based on submarine data from the central Arctic region, Rothrock et al. (1999) found a decline in

Arctic sea ice draft, the part of the ice below the water level, of 1.3 m from the 1960s to the 1980s. Over the last decade both laser and radar altimeters have been used to estimate sea ice thickness on a basin-wide scale (Laxon et al., 2003; Kwok et al., 2004). Analysing measurements from the laser altimeter onboard ICESat, Kwok et al. (2009) found a decline in Arctic sea ice thickness of $0.18\,\mathrm{m\,a^{-1}}$ between 2003 and 2008. Spatially the strongest decline was found in the region covered by multi-year ice between Greenland and the North Pole. These results were consistent with sea ice thickness estimates from ERS and EnviSat radar altimeters reporting strong inter-annual variability in sea ice thickness (Laxon et al., 2003), and circumpolar thinning of Arctic sea ice following the 2007 record ice extent minimum (Giles et al., 2008). Combining sea ice thickness estimates from satellites and submarines, Kwok and Rothrock (2009) determined that, in the central Arctic where submarine data were released, the mean ice thickness in autumn declined from 3.02 m in the 1960s to 1.92 m in the 1990s, and then to 1.43 m during the 2003–2007 ICESat period.

Sea ice thickness is a quantity that cannot be measured directly by satellite-based instruments. Altimeters on board satellites measure the elevation of the Earth's surface, and by identifying leads between the ice floes, the freeboard (the height of the ice above the water level) can be derived. The thickness is calculated by assuming hydrostatic equilibrium and estimating the density of sea ice and snow and the snow depth on top of the ice. These quantities may vary both in space and time and introduce large uncertainties in the sea ice thickness estimates.

Decline in sea ice area and thickness results in a reduction of sea ice volume. Based on data from the laser altimeter onboard ICESat, Kwok et al. (2009) found a net loss of 5400 $\mathrm{km^3}$ in October/November and 3500 $\mathrm{km^3}$ in February/March during the ICESat record from 2003 to 2008. Recent results, exploring new data from the radar altimeter onboard CryoSat-2, report a further decline in Arctic sea ice volume (Laxon et al., 2013). The average sea ice volume in October/November for 2010 and 2011 was estimated to be 7560 $\mathrm{km^3}$, i.e. 64 % of the 2003–2008 mean value estimated from ICESat (Kwok et al., 2009). For the maximum annual value in February/March, the sea ice volume was estimated to be 14 819 $\mathrm{km^3}$, i.e. 91 % of the previous ICESat value (Laxon et al., 2013).

To investigate the influence of snow depth, sea ice density, and area on sea ice thickness and volume estimates we use freeboard retrievals from ICESat, together with different assumptions about snow and ice properties, and sea ice concentration derived from different algorithms. Uncertainties are calculated with a Monte Carlo approach based on probability distribution functions for the three parameters. Our approach is different to earlier methods as we take into account the spatial auto-correlation of uncertainties. We also provide, for the first time on an Arctic-wide scale, contributions of each of the analysed parameters to the total volume uncertainty. Our paper is outlined as follows: in Sect. 2 we describe the data sets used for ice sea freeboard, area, type and snow depth. In Sect. 3 we describe how sea ice thickness is estimated and provide a description of the Monte Carlo approach used to calculate uncertainties in sea ice thickness and volume. Results on the uncertainties in sea ice thickness and volume are given in Sect. 4, and a detailed discussion, including implications of the trend in sea ice volume, is given in Sect. 5.

2 Data

To calculate sea ice thickness and volume, we combine satellite-based retrievals of sea ice freeboard, type and area. In this section we will describe the data sets and the processing steps used to derive the necessary parameters for our analysis.

2.1 Sea ice freeboard

The starting point of this paper is the ICESat freeboard retrieval. The Geoscience Laser Altimeter System (GLAS) on ICESat uses a 1064 nm laser channel for surface altimetry, with an expected accuracy of 15 cm. The satellite orbit has an inclination of 94°, measurements have a resolution of 70 m, and the surface was sampled every 170 m (Zwally et al., 2002). ICESat was in orbit for almost six years from 2003 to 2009, but was generally operating only for two separated periods each year in February/March and October/November. The laser measures the top of the snow on the ice, if snow is present, and the freeboard value retrieved is thus the combined value for sea ice and snow.

The data set mainly used in our study is available from NSIDC (Yi and Zwally, 2009) and based on the original data processing described by Zwally et al. (2002). The data set is only available for the campaigns from October/November 2005–2007 (see Table 1 for more information) and provides sea ice freeboard information along the track. Sea ice thickness is also available in this data set but has not been used in our analysis. In this algorithm the freeboard has been obtained by defining leads as the lowest 1 % of elevation along a 50 km running mean. Further detail on the original processing and the freeboard retrieval are provided in Zwally et al. (2002) and at NSIDC (http://nsidc.org/data/docs/daac/nsidc0393_arctic_seaice_freeboard/index.html, Yi and Zwally, 2009).

For comparison we also use the gridded sea ice thickness data set from JPL (available at http://rkwok.jpl.nasa.gov/icesat/download.html). To get information about sea ice freeboard a slightly different approach has been used for this data set. Kwok et al. (2007) used the standard deviation of surface elevation together with values of reflectivity to identify leads. Additionally, Kwok et al. (2009) included two corrections to account for possible unresolved biases, such as due to the size of leads and snow accumulation on refrozen

Table 1. ICESat campaigns as used in this study.

Survey	Period
ON05	21 Oct to 24 Nov 2005
FM06	22 Feb to 27 Mar 2006
ON06	25 Oct to 27 Nov 2006
MA07	12 Mar to 14 Apr 2007
ON07	2 Oct to 5 Nov 2007

leads. A detailed description of this data set can be found in Kwok and Cunningham (2008) and Kwok et al. (2009).

As no freeboard data are available from JPL, we did not perform an analysis of freeboard uncertainties. In our study we focus on how snow depth, sea ice density, and area influence sea ice thickness estimates. In this way the word "uncertainty" as used in this study covers the "geophysical assumptions" about the sea ice thickness estimate and not instrumental "errors". A detailed analysis of the freeboard retrievals and its associated uncertainties for each algorithm were described in a clear and concise manner by Zwally et al. (2002), Kwok et al. (2007), and Kwok and Cunningham (2008).

2.2 Sea ice type

Information about sea ice type is derived from QuikSCAT scatterometer data. QuikSCAT provides normalised radar cross section ($sigma_0$) measurements of the Earth's surface. In this study we use daily averaged gridded QuikSCAT data processed at Brigham Young University (BYU) for each midday of the evaluated periods (ftp://ftp.scp.byu.edu/data/qscat/SigBrw). The small hole around the North Pole (0.5° N) is filled with a nearest neighbour interpolation. Backscatter is converted into a multi-year ice (MYI) fraction using the method described in Kwok (2004). This method is based on a relationship between the MYI fraction from high-resolution RADARSAT/RGPS images and $sigma_0$ backscatter from QuikSCAT (see Fig. 6 in Kwok, 2004). We checked that our results are consistent with the fields published in Kwok (2004) and Polyakov et al. (2011) for 1 January 2000–2008.

The backscatter from scatterometers is sensitive to the physical properties of sea ice that change after sea ice has survived the melting season. Thus the term MYI, as defined in this study, refers to sea ice that has survived one summer, but may actually be younger than one year. However, as scatterometers only capture the surface properties, this method does not allow us to account for the part of first-year ice (FYI) growing from the bottom during winter freezing, and therefore underestimates the volume fraction of FYI.

In this study we use two different approaches to define the sea ice type: a fraction of the ice type per pixel, as described above, and a binary classification. To get the binary sea ice classification between FYI and MYI for each pixel we used a threshold of 50 % for the sea ice type. This binary classification has been used in previous studies, e.g. Kwok et al. (2009).

2.3 Sea ice area

Sea ice area is derived from sea ice concentration estimates based on brightness temperatures from DMSP SSM/I (Special Sensor Microwave Imager). In this study, we use gridded brightness temperatures in polar stereographic projection available from NSIDC (Maslanik and Stroeve, 2004, updated 2012). Various algorithms exist to derive sea ice concentration from this type of measurement. The underlying theory behind the algorithms is that sea ice and open water emit differently across the frequency spectrum and polarisations. The measured brightness temperatures are therefore a linear combination of these two temperatures, with weights according to the concentration of sea ice and water. Algorithms differ due to the use of different frequencies and tie points for ice and water, and are sensitive to changes in the physical temperature of the surface and weather filters (Comiso et al., 1997). Ice concentration products used in this study are based on 11 different algorithms and are listed in Table 2.

2.4 Snow depth

Our knowledge of snow depth on top of Arctic sea ice is limited. Snow depth can be measured directly in the field, but these measurements are limited to field campaigns in a local area during a couple of weeks. The most comprehensive compilation of in situ data so far is based on man-made observations taken during Soviet drifting stations between 1954 and 1991. Warren et al. (1999, W99 hereafter) created a climatology of monthly snow depth by fitting a two-dimensional quadratic function for each month independently of the year. The mean winter (October–April) snow depth from W99 is shown in Fig. 1 as thin contour lines. Because MYI was the dominating ice type during those decades, the climatology represents snow depth on MYI.

Another way to obtain information about snow depth on a basin-wide scale are retrievals from passive microwave sensors (Markus and Cavalieri, 1998). In this case snow depth is calculated using the spectral gradient ratio of the 18.7 and 37 GHz vertical polarisation channels. In our study we use the data sets based on AMSR-E (Markus and Cavalieri, 2008) for which the algorithm is applied over FYI. Evaluation studies found the retrieval to be accurate over smooth first-year ice, while over rougher FYI or MYI it needs further development (Markus et al., 2006; Brucker and Markus, 2013).

In our freeboard estimates we require that the freeboard should always be positive. Negative freeboard as a result of e.g. ice flooding is common in Antarctica due to the large snowfall in that region (Lytle and Ackley, 2001), but this has not been observed to a large degree in the Arctic. We therefore replaced the snow depth with the freeboard value

Table 2. Sea ice concentration algorithms used to calculate the influence of sea ice area on estimates of sea ice thickness and volume.

Algorithms	Reference
NORSEX	Svendsen et al. (1983)
NASA Team	Cavalieri et al. (1984)
UMass-AES	Swift et al. (1985)
Bootstrap	Comiso (1986)
Near90 GHz	Svendsen et al. (1987)
CalVal	Ramseier (1991)
Bristol	Smith and Barrett (1994)
NORSEX-85H	Kloster (1996)
TUD	Pedersen (1998)
NASA Team 2	Markus and Cavalieri (2000)
ASI	Kaleschke et al. (2001)

in the cases where the snow depth was larger than the freeboard.

3 Methods

To combine the data sets we described above, we re-gridded them following a polar stereographic projection onto a 25 km grid. For snow depth we used the mean value of the two periods, in autumn and late winter (see Table 1), when freeboard measurements were available. For sea ice area we used the mean over each ICESat period and for the MYI fraction the mid-day of each ICESat period. As the export of MYI is only about 10 % each year (Smedsrud et al., 2011) we believe that the change in MYI fraction is slow enough to allow for this simplification.

ICESat has an orbit inclination of 94°, hence for a considerable percentage of the Arctic Ocean, no freeboard measurements are available. To fill this data gap we use the MYI fraction around the hole as a proxy for sea ice thickness. For each ICESat period, we fitted a third-order polynomial to the values of sea ice thickness and an MYI fraction 2 degrees around the data hole, and used this function to derive information about sea ice thickness within the hole. A similar method has previously been used by Kwok et al. (2009) and provides a simple way to get an estimate of sea ice thickness and volume on a basin-wide scale. Other data gaps, mostly occurring in the shelf areas, have been filled similarly, using the fraction of MYI in the adjacent pixels. As done in previous studies, all results presented in our analysis are restricted to the "ICESat domain", which does not include the Canadian Archipelago, the Fram Strait, or the Bering, Barents and Kara seas.

3.1 Sea ice thickness estimates

To convert sea ice freeboard measurements from ICESat into sea ice thickness a number of assumptions have to be made. The first major assumption is that sea ice floats in hydrostatic

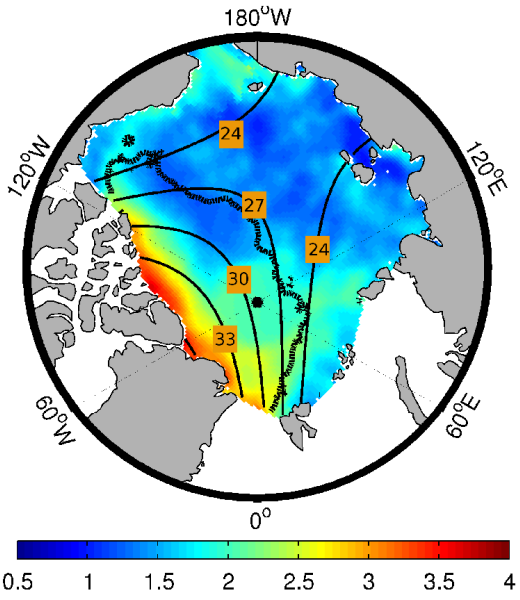

Fig. 1. Arctic sea ice properties and the Arctic sea ice area as defined in this study. Annual mean sea ice thickness from ICESat is shown in colour (m). The line of 50 % multi-year ice fraction is plotted as a thick contour line. Both parameters are given as the average during the 2005–2007 ICESat campaigns. Climatological winter (October–April) snow depth from Warren (1999) from 1954 to 1991 is given as the labelled thin contour lines in centimetres.

equilibrium, which results in the following equation for the sea ice thickness (SIT):

$$\mathrm{SIT} = f_{\mathrm{is}} \cdot \frac{\rho_{\mathrm{w}}}{\rho_{\mathrm{w}} - \rho_{\mathrm{i}}} + h_{\mathrm{s}} \cdot \frac{\rho_{\mathrm{s}} - \rho_{\mathrm{w}}}{\rho_{\mathrm{w}} - \rho_{\mathrm{i}}}, \quad (1)$$

where f_{is} is the snow ice freeboard as retrieved from ICESat, h_{s} is the snow depth, and ρ_{w}, ρ_{s}, and ρ_{i} are the densities of water, snow and ice, respectively. The thickness depends on the measured freeboard, and the snow and sea ice properties. For ρ_{w} we use a value of 1024 kg m^{-3} and for ρ_{s}, 270 kg m^{-3} in October/November and 330 kg m^{-3} in February/March, following Warren et al. (1999). To investigate the influence of ρ_{i} and h_{s} on sea ice thickness estimates on a basin-wide scale we analyse a number of data sets for these two parameters as described below in Sects. 3.2 and 3.3.

Equation (1) describes the "true" sea ice thickness, which is the averaged thickness of the ice in a certain area. An observer on the ice would think this is the most meaningful value of ice thickness. We also analyse the effective sea ice thickness, which is defined as the mean sea ice thickness including open water areas. We use the sea ice concentration to account for the open water in each pixel and compute the effective sea ice thickness as follows:

$$\mathrm{SIT}_{\mathrm{eff}} = \mathrm{SIT} \cdot \mathrm{SIC}\,[0, 1], \quad (2)$$

where $\mathrm{SIT}_{\mathrm{eff}}$ is the effective sea ice thickness, SIT is the sea ice thickness as described in Eq. (1), and SIC is the sea ice

concentration. This is the most common diagnostic in current sea ice models in which sea ice mainly grows thermodynamically and rather homogeneously over a grid cell.

3.2 Density scenarios

The density of sea ice depends on the amount of brine and air inclusions, and therefore on temperature and sea state during formation and the age of the ice. Ice containing no salt is expected to have a density of 916 kg m^{-3}. Newly frozen FYI, however, contains a substantial amount of salt water that increases the sea ice density. Concentrated sea water with a salinity higher than 35 is termed brine, and brine salinities can reach values up to 100 depending on the sea ice temperature. In the course of time the brine drains out and is replaced by air. Density of MYI is thus expected to be lower than that of FYI, in particular in the freeboard part above water level, and values vary greatly among the sources (e.g. Timco and Frederking, 1996; Kovacs, 1996; Alexandrov et al., 2010; Forström et al., 2011). To investigate and visualise the influence of sea ice density on sea ice thickness we explored different values ranging from 882 to 925 kg m^{-3} (see Table 3). We first assumed the sea ice density to be the same over the entire Arctic (D1–D4), and second we varied the sea ice density dependent on ice type (D5 and D6). For the second approach, we chose the ice type either by a binary classification (D5) or by accounting for the fraction of MYI per pixel (D6).

3.3 Snow depth scenarios

To assess the influence of snow depth on sea ice thickness estimates we used the snow depth retrieval from AMSR-E, and the W99 climatology. Additionally, we used a modification of W99 based on results from airborne measurements of snow depth. Evaluating snow depth data from the Operation IceBridge campaigns, Kurtz and Farrell (2011a) found that snow load is reduced by 50 % over FYI compared to climatological values of W99. An overview of our selected values is presented in Table 4. As for the ice density, we either used the same assumption over FYI and MYI (S1 and S5) or used different assumptions for the two ice types (S2–S4). Snow depth weighted by MYI fraction (S3) has been calculated as follows:

$$H_s = \mathrm{W99} \cdot (0.5 + 0.5 \cdot \mathrm{MYI}_{\mathrm{fraction}}), \quad (3)$$

where W99 is snow depth based on climatological values from Warren et al. (1999). The AMSR-E product is available over FYI, but the classification of sea ice type used is different from our approach. Therefore the pixels considered as FYI are slightly different than those based on the MYI fraction derived from QuikSCAT.

3.4 Monte Carlo approach to calculating uncertainty

The uncertainties regarding sea ice volume and thickness are calculated using a Monte Carlo approach. This is a probabilistic method based on repeated calculations of the results, using input parameters changed by a random selection from their probability distributions. Parameters and their uncertainties are therefore not simply treated as a mean value and its standard deviation, but for each input parameter real data, algorithms and distributions are used. In our study the result is the effective sea ice thickness (or sea ice volume) and the input parameters are sea ice area, density and snow depth. For sea ice area we assume each of the eleven algorithms to be equally likely (distribution not shown). The assumed PDFs of snow depth and sea ice density are shown in Fig. 2 and are described in detail in the paragraphs below. To calculate total uncertainties we iterate simultaneously through the PDFs of all three parameters according to their respective PDF. To calculate the uncertainty coming from a single parameter we iterate through the PDF of this parameter and keep the other two fixed at the mean value. As the cross-correlation between the parameters is not well understood, it is not included in our approach. Spatial auto-correlation for each parameter is included by varying the parameters Arctic wide for each Monte Carlo run, or according to its sea ice type.

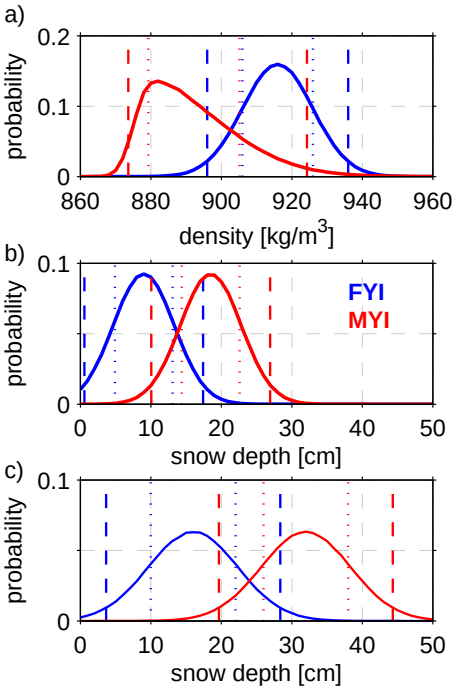

Fig. 2. Probability distributions for sea ice density and snow depth. Distributions are shown separately for first-year ice (FYI) and multi-year ice (MYI). **(a)** Mean sea ice density, **(b)** mean snow depth in October/November, and **(c)** mean snow depth in February/March. Snow depth over MYI is based on climatological values from W99, and 50 % of this snow depth is used over FYI. Dotted lines indicate the first standard deviation (15 and 85 percentile) and dashed lines the second standard deviation from the mean (2.3 and 97.7 percentile).

Table 3. Different assumptions about sea ice density as used in this study to assess the possible range of sea ice thickness.

Acronym	Sea ice density [kg m^{-3}]		Description	Used e.g. in
D1	916		Typical value found for FYI	Similar to Laxon et al. (2003) and Alexandrov et al. (2010)
D2	925		Density of ice containing brine inclusions	Kwok et al. (2009) (JPL data set)
D3	882		Density of ice containing air inclusions Typical value found for MYI	Alexandrov et al. (2010)
D4	900		mean value	
	FYI	MYI		
D5	916	882		Laxon et al. (2013)
D6	916	882	Weighted by MYI fraction in each pixel	

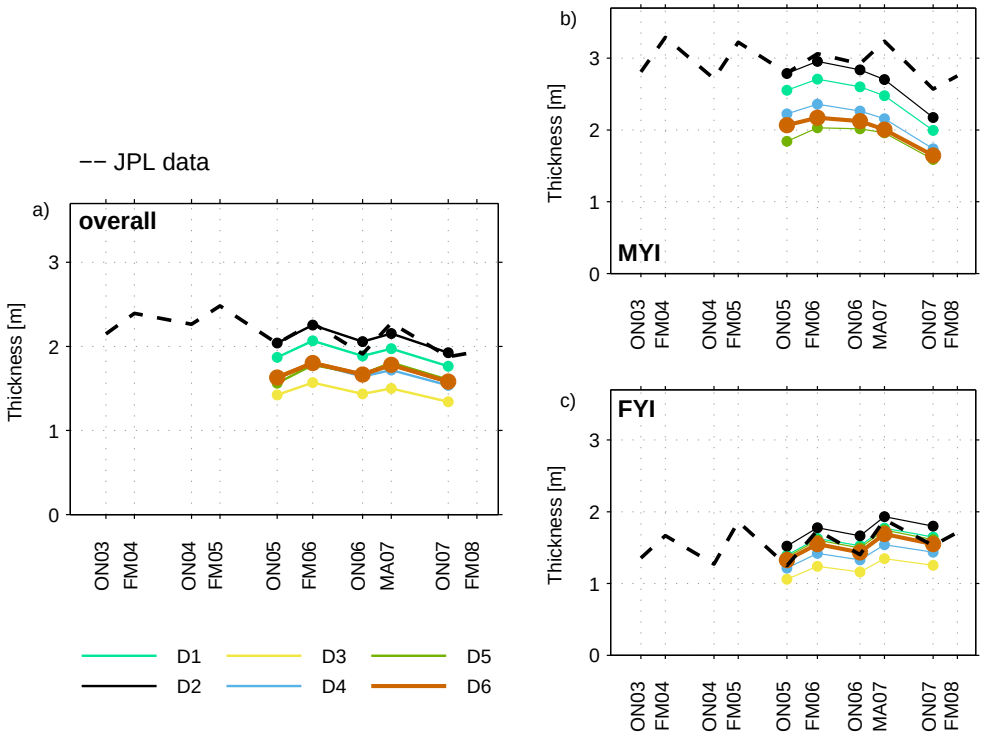

Fig. 3. Spatially averaged Arctic sea ice thickness calculated with different values for ice density. In **(a)** the total mean thickness is shown, in **(b)** the thickness of multi-year ice (MYI) and in **(c)** the thickness of first-year ice (FYI). Density values used are described in Sect. 3.2 and can be found in Table 3. The brown line (D6) is the same as S3 in Fig. 5.

The PDF of snow depth follows the W99 climatology over MYI and is reduced by 50 % over FYI. For the standard deviation of the distributions we use the reported inter-annual variability from the W99 climatology, of i.e. 4.3 cm in October/November and 6.2 cm in February/March. This is consistent with uncertainties found for the AMSR-E retrieval (Brucker and Markus, 2013), so we believe that our assumptions are still conservative. In Fig. 2 we show separate distributions for MYI and FYI for visualisation, but in reality the correlation between snow depth on FYI and MYI has to be considered. For each Monte Carlo calculation we therefore picked one random value from the MYI distribution and took half of this value for the FYI. For the campaign in spring 2007 we used a PDF which was one centimetre higher than shown in Fig. 2, because the campaign took place in March/April. Because snow depth can not be negative we set a lower bound at 0 cm.

For the PDF of sea ice density we also assumed different values for FYI and MYI. For FYI we assumed a mean value of 916 kg m^{-3} and a standard deviation of $\pm$10 kg m^{-3} which is smaller than reported in other studies (Alexandrov et al., 2010; Forström et al., 2011). For the Monte Carlo approach

we seek a value that would correspond to a basin-wide average over a number of years, while the reported values are based on field observations from a local area and a given time. For the MYI density we assume a slightly skewed distribution as MYI generally includes areas of FYI, both from bottom freezing and refrozen leads, and literature values vary widely among the sources. The mode of the density distribution is 882 kg m^{-3}, while the mean is slightly higher, i.e. 890 kg m^{-3}.

4 Results

In this section we first illustrate the influence of selected values for density and snow depth on the sea ice thickness estimates. We further show uncertainties in effective sea ice thickness due to sea ice area, density and snow depth, and how they are distributed over space and time. Finally we use these estimates to calculate the total sea ice volume and its uncertainties, and show implications for reported trends in sea ice volume.

4.1 Sea ice density influence on sea ice thickness

Mean sea ice thickness calculated over the whole Arctic basin using different assumptions about sea ice density is shown in Fig. 3. The assumptions are listed in Table 3. The same snow depth was used for all calculations, and corresponds to climatological values from W99 over MYI, and half of the values over FYI weighted by MYI fraction per pixel (S3 in Table 4).

We show that the mean sea ice thickness is strongly influenced by the choice of sea ice density, while the trend and the annual cycle are hardly affected. The resulting mean values in October/November range between 1.39 and 2.00 m. At the end of winter, in February/March sea ice thickness has increased and ranges between 1.53 and 2.20 m. Because the influence of sea ice density increases with sea ice thickness, we found the range to be smaller for FYI (about 55 cm), and larger for MYI (about 80 cm). The difference in sea ice density due to different sea ice classification methods only influences the mean sea ice thickness by a few centimetres, and the difference between D5 and D6 in Fig. 3 is too small to be visible.

The trend in FYI and MYI thickness is diametric: while the thickness of MYI decreases over the period (Fig. 3b), the thickness of FYI increases (Fig. 3c). A number of processes could contribute to such an increase in thickness and we will come back to these in the discussion section.

From October/November to February/March the FYI thickness increases by about 0.25 m, representing "normal winter growth" over areas that were open water at the beginning of the freezing season. However, it is surprising and rather counterintuitive to see that the mean thickness of MYI does not increase between October/November 2006 and February/March 2007 (Fig. 3b). To get more insight into this peculiarity and the inter-annual variability we proceed with analysing the impact of snow depth on the mean sea ice thickness estimates.

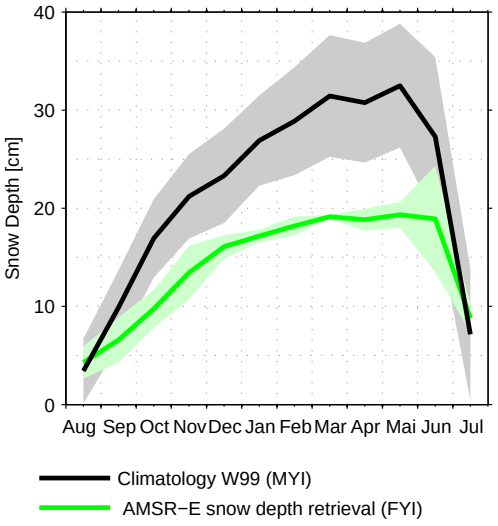

Fig. 4. Annual evolution of the spatially averaged snow depth on the Arctic sea ice. The spatial pattern is shown in Fig. 1, and the W99 climatology is based on observations between 1954 and 1991 of multi-year ice (MYI). The AMSR-E snow depth retrievals cover first-year ice (FYI) and is averaged for the IceSat period between 2003 and 2008. For both data sets the standard deviation is plotted around the mean value of any given month.

4.2 Snow depth estimates over Arctic sea ice

Figure 4 compares the climatology from W99 representing snow depth on MYI, and the snow depth retrieval from AMSR-E over FYI. Based on the W99 climatology the mean snow depth on the Arctic sea ice increases from near zero in August to a maximum in spring. The accumulation rate is as high as 5 cm month^{-1} from August to January, before lowering to about 2 cm month^{-1} until March. The snow increases somewhat further until May, before solar radiation is strong enough to melt the snow in June and July. At the end of summer only a few cm of snow are left. The inter-annual variability in the W99 climatology ranges from 3 to 8 cm, and is largest in the winter period.

Based on the AMSR-E snow depth retrieval the snow accumulation over the winter season has a similar shape, with a maximum in late winter, in phase with the W99 climatology. The accumulation rate, however, is much lower and the maximum value of about 19 cm is only 54 % of the climatological value from W99. One can speculate that this is not only a result of snow falling into water, but is additionally caused by changed atmospheric conditions and a reduction in snowfall (Screen and Simmonds, 2012). These might also have influenced the snow depth on MYI and can

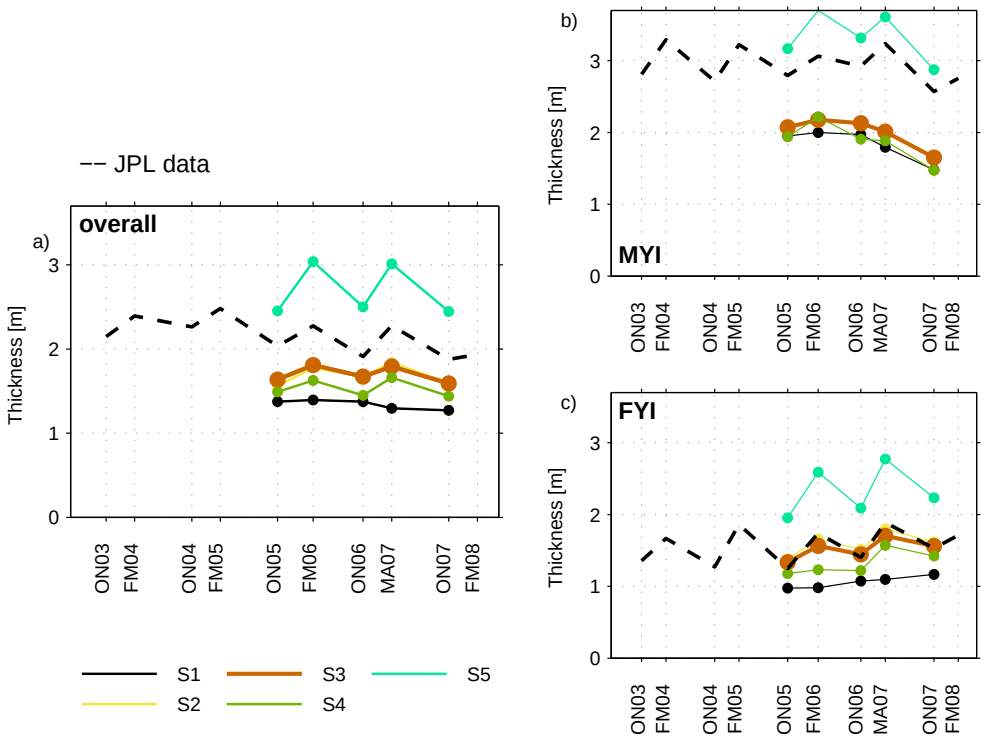

Fig. 5. Spatially averaged Arctic sea ice thickness calculated with different assumptions about snow depth. In **(a)** the total mean thickness is shown, in **(b)** the thickness of multi-year ice (MYI) and in **(c)** the thickness of first-year ice (FYI). Values are based on the available data sets described in Sect. 4.2, and can be found in Table 4. The brown line (S3) is the same line as D6 in Fig. 3.

Table 4. Different assumptions about snow depth as used in this study to assess the possible range of sea ice thickness due to snow depth.

Acronym	Snow depth		Description	Used e.g. in
	FYI	MYI		
S1	W99	W99	Snow taken from climatology W99	Laxon et al. (2003), Giles et al. (2008)
S2	W99/2	W99		Laxon et al. (2013)
S3	W99/2	W99	Weighted by MYI fraction in each pixel	
S4	AMSR-E	W99	Snow depth retrieval from AMSR-E used over FYI	
S5	0	0	Lowest possible value	

explain some of the peculiarities mentioned in the previous section. The absence of MYI thickening between October/November 2006 and February/March 2007 (Fig. 3b) could partly be explained by an overestimation of snow depth in February/March, which results in an underestimation of sea ice thickness. More information about the influence of snow depth on sea ice thickness estimates is given in the next section.

4.3 Snow depth influence on sea ice thickness

Mean sea ice thickness calculated from ICESat freeboard observations over the whole Arctic Ocean using different assumptions about snow depth is shown in Fig. 5. The different assumptions are given in Table 4. For sea ice density we used the ice type-dependent method (D6 in Table 3) weighted by MYI fraction per pixel.

Mean sea ice thickness in October/November ranges between 1.28 and 2.45 m, but goes down to 1.62 m if we exclude the "no snow" assumption, which is unrealistic but still considered as a reference. In February/March the mean sea ice thickness ranges between 1.33 and 3.00, or 1.79 m if the no-snow assumption is left out. The effect of sub-grid scale variability of snow depth due to sea ice type is about a few cm only (compare S2 and S3 in Fig. 5), which is similar to the results found for the sub-grid scale variability of ice density (Fig. 3).

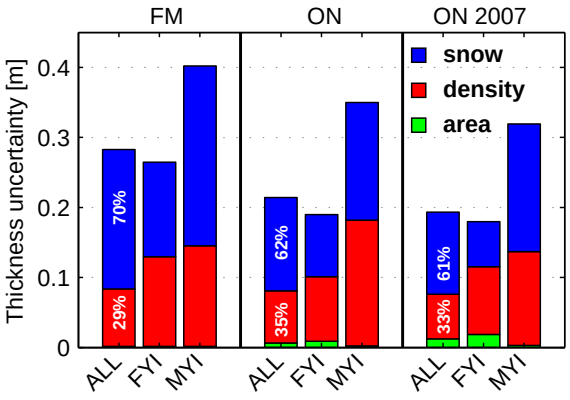

Fig. 6. Absolute uncertainties of the effective sea ice thickness. Contributions from uncertainties in sea ice density, snow depth, and sea ice area are included and given for the mean in February/March (FM) and October/November (ON). Additionally, October/November 2007 (ON07) is shown separately. Note that the distributions of sea ice density and snow depth are non-Gaussian for the total sea ice (see PDFs in Fig. 2) and therefore the contributions from the three parameters over first-year ice (FYI) and multi-year ice (MYI) do not sum up for the total sea ice thickness (ALL).

Using climatological snow depth from W99 for FYI, we found no increase in sea ice thickness in the winter season (S1 in Fig. 5). This is a counterintuitive and an unrealistic result, indicating that the W99 snow depth needs revision, as sea ice is indeed expected to increase in thickness during an Arctic winter. Reducing the climatological values from W99 by half or using available passive microwave retrievals from AMSR-E over FYI results in an increase in winter growth to about 40 cm (S2–S4 in Fig. 5).

For MYI we can only use the W99 climatology for snow depth, as no other data sets are available. The resulting spread in Fig. 5b is due to the different MYI classifications in the retrievals. As mentioned above, the absence of MYI thickening between October/November 2006 and February/March 2007 (Fig. 3b) could be a result of an overestimation of snow depth in February/March.

4.4 Spatial distribution and absolute uncertainties

So far we have shown the range of spatially averaged sea ice thickness estimates over the Arctic Ocean as the results of different selected values for sea ice density and snow depth. To get more insight into how the uncertainties in ice density, snow depth and sea ice area contribute quantitatively to the total uncertainty in the sea ice thickness estimates, we introduce results from the Monte Carlo approach. As the sea ice area is considered now, the results represent uncertainties in the effective sea ice thickness. The individual uncertainties are calculated keeping two of the parameters fixed at the mean values, while varying the third according to the PDFs shown in Fig. 2. We used the MYI fraction in each pixel when calculating the ice type-dependent values for sea ice density and snow depth (see Eq. 3).

Averaged absolute uncertainties and the contributions from sea ice density, snow depth, and sea ice are shown in Fig. 6. Mean absolute uncertainty of effective sea ice thickness is close to ± 0.25 m for each ICESat campaign. It is smaller in October/November (± 0.21 m) than in February/March (± 0.28 m), and we found snow depth to be the largest contributor to the total uncertainties with up to 70 %. Ice density contributes 30–35 %, with higher values in October/November due to the small snow cover at that time of year. The area contribution also increases in October/November but remains below 10 %.

The spatial distributions of these uncertainties in absolute values and their relative contribution to the total uncertainties are shown in the maps of Fig. 7. We only show results for October/November, but the spatial distribution of uncertainties is very similar in winter. Overall, the absolute uncertainty resulting from sea ice density is around 0.1–0.2 m for FYI, with uncertainties increasing for the thicker sea ice between the North Pole and Greenland (Fig. 7a). The transition from FYI to MYI also marks the transition from the smaller to the larger uncertainties, stemming from the larger uncertainty in density for MYI that we assumed in our analysis (see Fig. 2). For MYI the uncertainties in the sea ice thickness estimates resulting from sea ice density are therefore up to 70 %, while over FYI its relative contribution remains mostly below 40 %.

The absolute uncertainties resulting from uncertainties in snow depth show a similar pattern, with smaller values for thin FYI (from 0.1 m) and increasing for the thicker part between the North Pole and Greenland to 0.25 m. The relative contribution from uncertainties in snow depth accounts for only about 40 % of the total uncertainty for the MYI but up to more than 70 % for FYI.

Uncertainty in effective sea ice thickness resulting from the different sea ice area algorithms is less than 5 %, or 10 cm (Fig. 7c). This is caused by the high ice concentrations inside our selected Arctic Ocean area of interest (Fig. 1). When ice concentrations approach 100 %, there is little difference between the algorithms, and the related uncertainties become small. Some larger values are visible in Fig. 7c in the marginal ice zone north of Svalbard and in the vicinity of the Bering Strait. In these locations the uncertainties in sea ice area drive the relative uncertainty in effective thickness up to 60 %. However, in this region the sea ice is very thin and concentrations are low; the large values therefore hardly contribute to the uncertainty in mean effective sea ice thickness and volume (Fig. 6).

4.5 Sea ice volume uncertainties

The evolution of sea ice volume over time and the related uncertainties calculated using a Monte Carlo approach are shown in Fig. 8. We estimate the mean Arctic sea ice volume

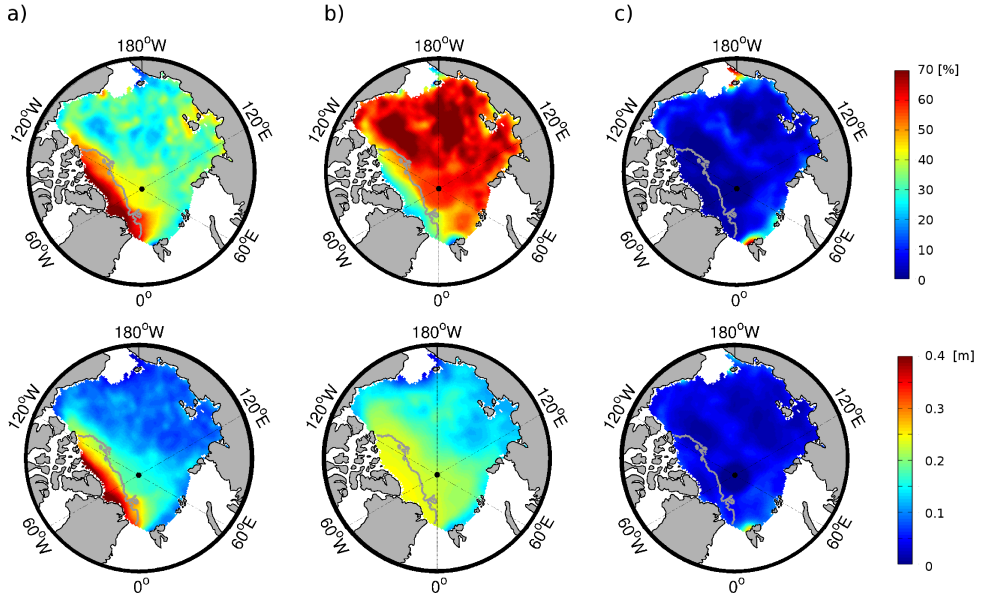

Fig. 7. Spatial distribution of uncertainties in effective sea ice thickness in October/November as a result of uncertainties in **(a)** sea ice density, **(b)** snow depth, and **(c)** sea ice area. The grey contour line indicates the 50 % multi-year ice fraction. In the upper line relative values of the total uncertainties are shown, and in the lower line absolute values of uncertainty.

between 2005 and 2007 to be $10\,120 \pm 1280\,\mathrm{km}^3$ in October/November, and to increase to $13\,250 \pm 1860\,\mathrm{km}^3$ in February/March (see green curve in Fig. 8).

The ice volume in October/November 2007 stands out as a major anomaly, following the steady reduction in MYI for the length of our record, and a large decrease in FYI volume since February/March 2007. The loss of FYI ice volume from February/March 2007 to October/November is more than 50 %, or about $4700\,\mathrm{km}^3$. This is especially remarkable as FYI volume actually increased from October/November 2005 until February/March 2007. In October/November 2005 MYI was the dominant ice type, but lost almost 50 %, or $\sim 3000\,\mathrm{km}^3$, of its volume by 2007. Because of this decrease, relative uncertainties in sea ice volume increase, and exceed 30 % at the end of the analysis period.

Absolute uncertainties and the relative contributions arising from uncertainties in sea ice density, snow depth and sea ice area are shown in Fig. 9. In February/March 73 % of the uncertainty is caused by uncertainties in snow depth. The snow contribution reduces to 55 % in October/November because of the thinner snow cover during this time of the year, similar to the absolute uncertainties for thickness (Fig. 6). Density thus plays a larger role during October/November but remains smaller than uncertainties resulting from uncertainties in snow depth. The sea ice area contribution is visible in October/November, but remains small throughout. This is however dependent on the area covered by sea ice, and particularly visible in October/November 2007, when it increases to around 5 %.

5 Discussion

We have calculated uncertainties in the estimates of Arctic sea ice thickness and volume. The uncertainties represented in this study arise from three different parameters that are set up when estimating sea ice thickness and volume: sea ice density, snow depth and sea ice area. Below we will first discuss the findings for sea ice thickness and its uncertainties and then discuss our results for sea ice volume, its uncertainties, and implications for its recent trend.

5.1 Sea ice thickness

We found that the choice of sea ice density significantly changes the estimated mean sea ice thickness. Our mean sea ice thickness ranges from 1.45 to 2.09 m using a range for sea ice density in accordance with the values seen in the literature. While the density affects the mean sea ice thickness, the snow depth affects its annual cycle and the inter-annual variability. The W99 snow depth climatology results in a underestimation of winter growth and indicates that the climatology is outdated, also over MYI.

The range of densities we used captures the real ice density, but it remains an unresolved issue whether the density has changed, or will be changing, due to a change in sea ice type over the Arctic Ocean, or due to changing weather conditions like warming temperatures and later ocean freeze-up. The snow depth has already been affected by these changes (Hezel et al., 2012; Kurtz and Farrell, 2011a), and our study confirms that the climatological values from W99 do not represent the current snow conditions over the Arctic sea ice.

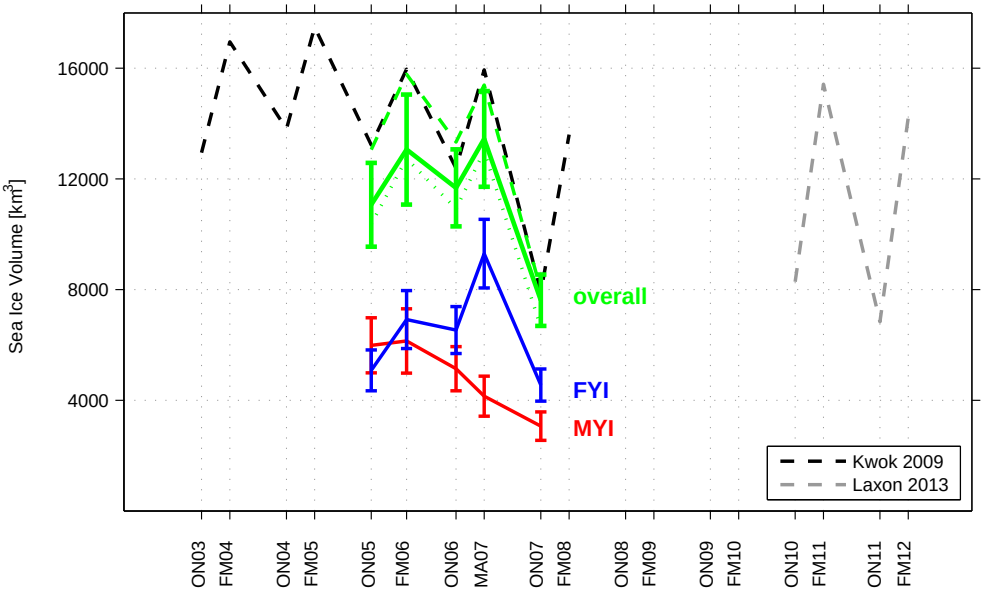

Fig. 8. Sea ice volume and its uncertainties calculated with different methods. For comparison ICESat results based on sea ice thickness data from JPL are included as a black dashed line, and CryoSat-2 values (Laxon et al., 2013) as the grey dashed line.

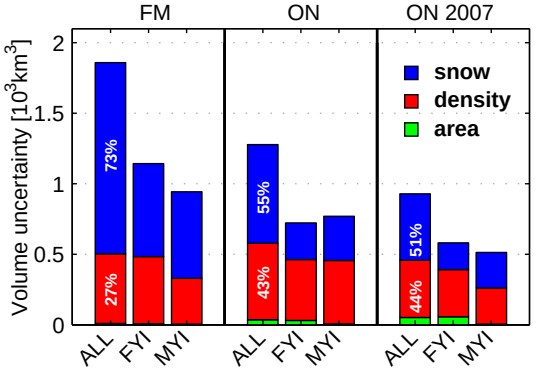

Fig. 9. Absolute uncertainties in Arctic sea ice volume. Contributions from uncertainties in sea ice density, snow depth, and sea ice area are included and given for the the mean in February/March (FM) and October/November (ON). Additionally, October/November 2007 (ON07) is shown separately. Note that the distributions of sea ice density and snow depth are non-Gaussian for the total sea ice (see PDFs in Fig. 2) and therefore the contributions from the three parameters over first-year ice (FYI) and multi-year ice (MYI) do not sum up for the total sea ice volume (ALL).

Absolute changes in snow depth do not have to be considered solely, but to derive accurate estimates for sea ice thickness, it is additionally important to capture its interannual variability. Passive microwave retrievals seem to be reliable over smooth FYI and have been found to be within ± 0.05 m of snow depth measurements from Operation IceBridge (Brucker and Markus, 2013). For large snow depths and rougher surfaces the uncertainties may however be larger (Markus et al., 2006). With thinning of the sea ice comes weakening and increased deformation (Rampal et al., 2009), so the retrievals may actually become less accurate in the future. Over MYI, the lack of more recent and accurate snow depth retrievals remains an issue, and explains why we have used the climatological values from W99 for this ice type in all our analyses. Recently, a new snow depth algorithm for thick ice has been developed (Maaß et al., 2013), based on brightness temperatures from the longwave passive microwave radiometer onboard SMOS. The algorithm requires more validation, but first results show very good agreement with airborne campaigns. The second way to retrieve information about snow depth on Arctic sea ice is to combine precipitation from atmospheric reanalysis and ice drift data from satellite products (used in e.g. Kwok and Cunningham, 2008; Kurtz et al., 2011b). The accuracy of the reanalysis data depends on the model set-up and the data assimilation method, which is not always reliable over the Arctic Ocean (Screen and Simmonds, 2011) and also varies significantly between different data sources (Bitz and Fu, 2008). Our results show that snow significantly affects the sea ice thickness estimates and an accurate method to retrieve snow depth will be essential to derive absolute values and trends in sea ice thickness in the future.

Using the Monte Carlo approach we estimate the mean absolute uncertainty of effective sea ice thickness to be ± 0.21 m in October/November and ± 0.28 m in February/March. Previous studies estimate the uncertainty in sea ice thickness to be e.g. 0.5 m (Kwok et al., 2009), 0.7 m (Kwok and Rothrock, 2009), 0.76 m (Giles et al., 2007), or 0.93 m (Forström et al., 2011). In all these studies the uncertainty has been calculated with the variance formula, which

is the common method for calculating uncertainties from uncorrelated parameters. The difference from our uncertainty estimates can be explained by two main reasons: our uncertainty estimates are for effective sea ice thickness and we did not include uncertainties resulting from freeboard and snow density. Freeboard has been found to be the main source of uncertainty and by not including it we clearly underestimate the uncertainties in sea ice thickness. However, the results are consistent with our findings that besides the freeboard, the snow depth is the main source of uncertainty. The different values found in the mentioned studies result from different assumptions made about the uncertainties of single parameters. In particular, there is large disagreement regarding the influence of snow density on the total uncertainty, ranging from 1 cm (Giles et al., 2007) to more then 20 cm (Kwok and Rothrock, 2009).

Sea ice thickness can also be estimated with sea ice models, which are an important tool for understanding and predicting the state of Arctic sea ice. Evaluating results from the Pan-Arctic Ice-Ocean Modeling and Assimilation System (PIOMAS), Schweiger et al. (2011) found a bias towards the ICESat-derived sea ice thickness estimates from JPL of 0.26 m in autumn and 0.1 m in spring. In spring this bias is within the range of our uncertainties, while in autumn it is slightly larger than uncertainties found in our study. Our analysis provides some possible explanations for the discrepancies found between the sea ice thickness estimates from ICESat and PIOMAS. Schweiger et al. (2011) found a larger difference between the two data sets north of Greenland and the Canadian Archipelago than in other areas, with ICESat giving values around 0.7 m larger than results from PIOMAS. As estimates from PIOMAS agree better with in situ data in this area, they hypothesised that ICESat retrievals may overestimate the sea ice thickness in this area of the Arctic Ocean. A part of this discrepancy could be explained by the choice of sea ice density. In the data set from JPL the sea ice density is chosen to be $925\,\mathrm{kg\,m^{-3}}$, and reducing it to $882\,\mathrm{kg\,m^{-3}}$ lowers the sea ice thickness by about 0.5 m (see Fig. 3). This explanation is supported by the apparently lower difference between sea ice thickness estimates from PIOMAS and CryoSat-2 (Laxon et al., 2013), where the reduced value for sea ice density has been used to convert freeboard into thickness. More comparison, however, is needed for verification.

5.2 Sea ice volume

We calculated the sea ice volume for the three years between 2005 and 2007 with a Monte Carlo approach using probability distribution functions for sea ice density, snow depth and area as described in Sect. 3.4. We estimate a mean sea ice volume of $10\,120 \pm 1280\,\mathrm{km^3}$ (12.7 %) in October/November, increasing to $13\,250 \pm 1860x\,\mathrm{km^3}$ (14 %) in February/March. In February/March snow depth accounts for more than 70 % of the uncertainty. In October/November, when snow depth is lower, the density becomes more important and accounts for 43 % of the total uncertainty.

These large uncertainties resulting from sea ice density can be illustrated using the selected values for the density as described in Sect. 3.2. Using a sea ice density of $925\,\mathrm{kg\,m^{-3}}$ as done in the JPL data set (see lines 2 and 3 in Table 5 and the green dashed line in Fig. 8) increases the sea ice volume by 15 % on a yearly average. Using values of 882 and $916.7\,\mathrm{kg\,m^{-3}}$, as done in Laxon et al. (2013) for the CryoSat-2 data, produces a sea ice volume about 5 % smaller than our Monte Carlo based volume estimates (see the green dotted line in Fig. 8 and line 4 in Table 5).

ICESat data have been freely available and have therefore been analysed in many studies (e.g. Spreen et al., 2006; Kwok and Cunningham, 2008; Farrell et al., 2009; Kurtz et al., 2011b; Schweiger et al., 2011). Only a minority of them, however, conducted detailed calculations of uncertainties and errors. A detailed but completely different approach to calculating the uncertainty in sea ice volume based on ICESat data was used by Kwok et al. (2009). The uncertainty was calculated as the sum of uncorrelated errors for each pixel: $\sigma_\mathrm{T} = N^{1/2}\left(A_\mathrm{c}^2\sigma_\mathrm{h}^2 + h^2\sigma_{A\mathrm{c}}^2\right)^{1/2}$, where σ_h and σ_{A_c} are the uncertainties in cell thickness (h) and cell area (A_c), σ_T uncertainties in total thickness, and N the number of grid cells. Assuming an error of 0.5 m for sea ice thickness, the resulting sea ice volume uncertainty in this study was given as $33\,\mathrm{km^3}$. This approach is valid for uncertainties in sea ice thickness stemming from uncorrelated errors, and as stated by Kwok et al. (2009), should be considered as a best case scenario. In our analysis we did not account for such uncorrelated errors, but uncertainties resulting from the mean values of snow depth, sea ice density and area. The uncertainties in these geophysical parameters should be understood more as a bias – not as uncorrelated errors. This explains why our ice volume uncertainty becomes as high as $\pm 1860\,\mathrm{km^3}$ in February/March, a value 56 times higher than the uncertainty calculated by Kwok et al. (2009). In the future more work needs to be done to analyse to which extent parameters and their uncertainties are correlated and to which extent retrieval errors are indeed random as assumed by Kwok et al. (2009). Both would lower the estimates of uncertainty. However, considering the lack of current knowledge of the absolute values, our uncertainty estimates can be assumed to be in the right range.

A bias in sea ice thickness as a measure of uncertainty that propagates into the estimates of uncertainty in sea ice volume has been previously used to assess uncertainties in modelled Arctic sea ice volume with PIOMAS (Schweiger et al., 2011). This is comparable to the uncertainties in our studies, and the resulting uncertainties in sea ice volume of 6.3 % in spring and 10 % in autumn are of the same order (14 and 12.7 % in our study for the two seasons, respectively). While Schweiger et al. (2011) used the differences between model results and validation data to identify the

Table 5. Sea ice volume as calculated in this study using different assumptions about the density in comparison with previous publications. Values that are calculated in this study are marked in bold. Same values are given in Fig. 8.

Source	Volume [km^3]	
	Oct–Nov	Feb–Mar
Monte Carlo mean	**10 120**	**13 254**
JPL data 2005–2007[b]	**11 705**	**14 842**
$\rho_i = 925\,kg\,m^{-3}$	**11 461**	**15 587**
$\rho_i = 916\,kg\,m^{-3}$ and $882\,kg\,m^{-3}$	**9312**	**12 870**
JPL data 2003–2008[b]	12 054	15 999
CryoSat 2010/11[a]	8283	15 424
CryoSat 2011/12[a]	6838	14 215

[a] Using $\rho_i = 916\,kg\,m^{-3}$ for FYI and $882\,kg\,m^{-3}$ for MYI.
[b] Using $\rho_i = 925\,kg\,m^{-3}$.

bias, in this study we provide additional physical insight, quantifying uncertainties resulting from geophysical parameters such as area, snow depth and sea ice density.

5.3 Implications for trends in sea ice volume

The calculated uncertainties have implications for trends in sea ice volume. Our time series of ICESat freeboard measurements from NSIDC is rather short, ranging from 2005 to 2007, which is admittedly too short to allow for robust calculations of trends. We therefore applied our calculated uncertainties of 12.7 % in February/March and 14 % in October/November to the longer time series processed at JPL (Kwok and Cunningham, 2008). Using a weighted regression to account for the obtained uncertainties (weighted by $1\,std^{-2}$), we calculate a trend of $-1450 \pm 530\,km^3\,a^{-1}$ in October/November and $-880 \pm 260\,km^3\,a^{-1}$ in February/March. The calculated trends are close to the previous findings from Kwok et al. (2009) of $-1240\,km^3\,a^{-1}$ in October/November and $-860\,km^3\,a^{-1}$ in February/March, respectively.

ICESat operated until 2008, and efforts to produce long-term trends by merging ICESat data with recent CryoSat-2 data are ongoing. Laxon et al. (2013) produced the first estimates and concluded on a loss of ice volume in October/November of $4290\,km^3$ between the mean of the ICESat period (2003–2008) and the CryoSat-2 period (2010–2012), which is a loss of about 36 %. In February/March they estimated a smaller loss of about $1480\,km^3$. In Table 5 we compare our results to the ICESat values from JPL (Kwok and Cunningham, 2008) and CryoSat-2 values from Laxon et al. (2013), illustrating the importance of the density estimate. Despite a consistent long-term change between ICESat and CryoSat-2 there are also differences that can be elucidated by our new results on uncertainties. The main difference is the high density of $925\,kg\,m^{-3}$ in the JPL data set used when converting freeboard measurements to thickness, compared to the values of 882 and $916\,kg\,m^{-3}$ used by Laxon et al. (2013) for CryoSat-2. Adjusting the values for sea ice density in the ICESat period accordingly (see Table 5) allows for a more consistent comparison between the ICESat and CryoSat-2 periods. For October/November this adjustment lowers the ice loss between the two periods considerably, and the ice loss becomes smaller than $2000\,km^3$, corresponding to a rate of $-390\,km^3\,a^{-1}$. For February/March we find that the Arctic ice volume has even increased from the end of the considered ICESat period 2007 up to March 2011.

The low loss, and in particular the increase, in sea ice volume between the ICESat and CryoSat-2 periods is an interesting and somewhat surprising result, raising questions about the accuracy of our methods. Indeed, the increase in February/March may partly be an artifact due to the snow depth assumed and the differences in the measurement techniques. The ice freeboard from ICESat is measured using a laser whose signal is reflected from the snow–air interface, while the radar signal from CryoSat-2 is assumed to be reflected from the snow–ice interface. Hence for ICESat data, more snow results in thinner sea ice, while for CryoSat-2 more snow results in thicker sea ice estimate. As stated above, the W99 climatology overestimates the snow depth on Arctic sea ice, not only over FYI (as previously found by Kurtz and Farrell, 2011a), but also over MYI. Therefore our estimates of ice thickness and volume from ICESat might be too low and estimates based on CryoSat-2 too high, which could artificially lead to the low loss, or increase, in ice volume between the two periods.

Sea ice thickness estimates from JPL (e.g. Kwok and Cunningham, 2008) and Laxon et al. (2013) have been evaluated and agree well with independent in situ data. Assuming that these data sets represent the real state of the Arctic sea ice, this implies that there are large biases in the freeboard retrievals and that these biases are mitigated by the choices made for sea ice density and snow depth. Biases can indeed be expected, in particular for CryoSat-2 due to preferential sampling of leads (Tonboe et al., 2010) or the unknown penetration depth of the radar signal into the snow layer (Willat et al., 2011). The evaluation data, however, are still highly limited in space and time, and do not cover all ice types and seasons. Therefore, more work is required to distinguish between the different, seasonally changing biases.

However, the moderate ice loss as found in our study in autumn is consistent with synoptic airborne measurements during summer, showing little change in sea ice thickness (Haas et al., 2010), and with satellite-based retrievals showing a slight recovery of the MYI fraction from 2008 till 2010 (Stroeve et al., 2012). On year-to-year timescales a temporal recovery of Arctic sea ice is indeed possible given e.g. an effective loss of insulation caused by the autumn snow ending in the ocean and not on the sea ice (Notz, 2009; Tietsche et al., 2011).

To get more robust results for long-term trends, further evaluation of the freeboard retrievals, in particular from CryoSat-2, is needed and more reliable estimates of sea ice density and snow depth on the Arctic sea ice are necessary. Our results indicate a less dramatic decline in Arctic sea ice volume than reported in previous studies, but it is not possible to draw quantitative conclusions about changes in sea ice volume between the ICESat period (2003–2008) and the CryoSat-2 (2010–2012) period.

6 Conclusions

Remotely sensed observations of Arctic sea ice thickness and volume are available for the last decade. In accordance with documented loss of sea ice area over the last 30 yr, available studies point to a dramatic loss of sea ice volume. We have shown here that such estimates of Arctic sea ice volume rest on a number of geophysical parameters that have influence on the overall mean, the year-to-year variability, and the trends. The overall uncertainties appear larger than previous studies suggest, and the dramatic ice loss appears smaller.

Despite the large number of algorithms available, and the associated uncertainties of ~ 1.3 million km^2, uncertainties in area do not carry over to the sea ice volume estimates in cold seasons over the Arctic Ocean. They become important when concentrations are well below 100 %, like in the marginal ice zone, and may therefore become more important in the future, caused by the ongoing sea ice retreat in the Arctic.

The choice of the mean density used when converting ICESat-derived freeboard measurements to sea ice thickness has a major influence on the resulting mean thickness, but does not alter the year-to-year variability. To obtain accurate estimates of changes in sea ice volume and thickness in the future, the change from mainly multi-year ice to first-year ice and the corresponding changes in sea ice density also have to be considered.

The snow loading on top of Arctic sea ice greatly effects the estimated thickness and volume during the winter and is a likely driver for year-to-year variability. Our results indicate that climatological values from Warren et al. (1999) not only overestimate the snow load on first-year ice compared to the present day climate, but also give incorrect values for multi-year ice.

The absolute uncertainty in mean effective sea ice thickness derived from the laser altimeter onboard ICESat is 0.28 m in February/March and 0.21 m in October/November. The uncertainty in snow depth contributes up to 70 % of the total error, and the ice density 30–35 %, with higher values in October/November.

We find large uncertainties in total sea ice volume and trend. For the total sea ice volume the mean is $10\,120 \pm 1280$ km^3 in October/November and $13\,250 \pm 1860$ km^3 in February/March for our time period from 2005 till 2007. We obtain a trend of -880 ± 260 km^3 a^{-1} in February/March and -1450 ± 530 km^3 a^{-1} in October/November in the ICESat period 2003–2008.

Our results still reveal a decline in sea ice volume between the ICESat (2003–2008) and CryoSat-2 (2010–2012) periods, but less dramatic than reported in previous studies. However, final quantitative conclusions about a change in sea ice volume are hard to make, considering the large uncertainties and unresolved biases found in our study.

Acknowledgements. We thank the editor Ron Lindsay and two anonymous reviewers for their critical comments and suggestions which helped us to improve the quality of our paper. We also acknowledge Laurent Bertino for his help on the statistical methods used for this study and Timothy Williams for language corrections. We thank the National Snow and Ice Data Center, University of Colorado, Boulder, USA for providing the input data for the sea ice concentration algorithms. This work is supported by the Research Council of Norway, through projects CISAR no. 202313/V30 and ArcticSIV no. 207584.

Edited by: R. Lindsay

References

Aagaard, K. and Carmack, E.: The role of sea ice and other fresh water in the Arctic circulation, J. Geophys. Res., 94, 14485–14498, doi:10.1029/JC094iC10p14485, 1989.

Alexandrov, V., Sandven, S., Wahlin, J., and Johannessen, O. M.: The relation between sea ice thickness and freeboard in the Arctic, The Cryosphere, 4, 373–380, doi:10.5194/tc-4-373-2010, 2010.

Bitz, C. M. and Fu, Q.: Arctic warming aloft is data set dependent, Nature, 455, E3–E4, doi:10.1038/nature07258, 2008.

Brucker, L. and Markus, T.: Arctic-scale assessment of satellite passive microwave derived snow depth on sea ice using operation IceBridge airborne data, J. Geophys. Res., 118, 2892–2905, doi:10.1002/jgrc.20228, 2013.

Cavalieri, D. J. and Parkinson, C. L.: Arctic sea ice variability and trends, 1979–2010, The Cryosphere, 6, 881–889, doi:10.5194/tc-6-881-2012, 2012.

Cavalieri, D. J., Gloersen, P., and Campbell, W. J.: Determination of sea ice parameters with the Nimbus 7 SMMR, J. Geophys. Res., 89, 5355–5369, doi:10.1029/JD089iD04p05355, 1984.

Comiso, J.: Characteristics of Arctic winter sea ice from satellite multispectral microwave observations, J. Geophys. Res., 91, 975–994, doi:10.1029/JC091iC01p00975, 1986.

Comiso, J. C., Cavalieri, D. J., Parkinson, C. L., and Gloersen, P.: Passive microwave algorithms for sea ice concentration: a comparison of two techniques, Remote Sens. Environ., 60, 357–384, doi:10.1016/S0034-4257(96)00220-9, 1997.

Farrell, S., Laxon, S., McAdoo, D., Yi, D., and Zwally, H.: Five years of Arctic sea ice freeboard measurements from the Ice, Cloud and land Elevation Satellite, J. Geophys. Res., 114, C04008, doi:10.1029/2008JC005074, 2009.

Forström, S., Gerland, S., and Pedersen, C.: Thickness and density of snow-covered sea ice and hydrostatic equilibrium

assumption from in situ measurements in Fram Strait, the Barents Sea and the Svalbard coast, Ann. Glaciol., 52, 261–271, doi:10.3189/172756411795931598, 2011.

Giles, K. and Hvidegaard, S.: Comparison of space borne radar altimetry and airborne laser altimetry over sea ice in the Fram Strait, Int. J. Remote Sens., 27, 3105–3113, doi:10.1080/01431160600563273, 2006.

Giles, K., Laxon, S., Wingham, D., Wallis, D., Krabill, W., Leuschen, C., McAdoo, D., Manizade, S., and Raney, R.: Combined airborne laser and radar altimeter measurements over the Fram Strait in May 2002, Remote Sens. Environ., 111, 182–194, doi:10.1016/j.rse.2007.02.037, 2007.

Giles, K., Laxon, S., and Ridout, A.: Circumpolar thinning of Arctic sea ice following the 2007 record ice extent minimum, Geophys. Res. Lett., 35, L22502, doi:10.1029/2008GL035710, 2008.

Haas, C., Hendricks, S., Eicken, H., and Herber, A.: Synoptic airborne thickness surveys reveal state of Arctic sea ice cover, Geophys. Res. Lett., 37, L09501, doi:10.1029/2010GL042652, 2010.

Hezel, P., Zhang, X., Bitz, C., Kelly, B., and Massonnet, F.: Projected decline in spring snow depth on Arctic sea ice caused by progressively later autumn open ocean freeze-up this century, Geophys. Res. Lett., 39, L17505, doi:10.1029/2012GL052794, 2012.

Kaleschke, L., Heygster, G., Lüpkes, C., Bochert, A., Hartmann, J., Haarpaintner, J., and Vihma, T.: SSM/I sea ice remote sensing for mesoscale ocean-atmosphere interaction analysis: ice and icebergs, Can. J. Remote Sens., 27, 526–537, 2001.

Kattsov, V. M., Ryabinin, V. E., Overland, J. E., Serreze, M. C., Visbek, M., Walsh, J. E.., Meier, W. and Zhang, X.: Arctic sea-ice change: a grand challenge of climate science, J. Glaciol., 56, 1115–1121, 2010.

Kloster, K.: Ice type concentration by microwave radiometry, Earth Observation Compendium for course AGF-207, Tech. rep., Norwegian Space Center, 1996.

Kovacs, A.: Sea Ice, Part 1, Bulk Salinity Versus Ice Floe Thickness, Tech. rep., DTIC Document, 1996.

Kurtz, N. and Farrell, S.: Large-scale surveys of snow depth on Arctic sea ice from operation IceBridge, Geophys. Res. Lett., 38, L20505, doi:10.1029/2011GL049216, 2011a.

Kurtz, N., Markus, T., Farrell, S., Worthen, D., and Boisvert, L.: Observations of recent Arctic sea ice volume loss and its impact on ocean-atmosphere energy exchange and ice production, J. Geophys. Res., 116, C04015, doi:10.1029/2010JC006235, 2011b.

Kwok, R.: Annual cycles of multiyear sea ice coverage of the Arctic Ocean: 1999–2003, J. Geophys. Res., 109, C11004, doi:10.1029/2003JC002238, 2004.

Kwok, R. and Cunningham, G.: ICESat over Arctic sea ice: estimation of snow depth and ice thickness, J. Geophys. Res., 113, C08010, doi:10.1029/2008JC004753, 2008.

Kwok, R. and Rothrock, D.: Decline in Arctic sea ice thickness from submarine and ICESat records: 1958–2008, Geophys. Res. Lett., 36, L15501, doi:10.1029/2009GL039035, 2009.

Kwok, R., Zwally, H., and Yi, D.: ICESat observations of Arctic sea ice: a first look, Geophys. Res. Lett, 31, L16401, doi:10.1029/2004GL020309, 2004.

Kwok, R., Cunningham, G., Zwally, H., and Yi, D.: Ice, Cloud, and land Elevation Satellite (ICESat) over Arctic sea ice: retrieval of freeboard, J. Geophys. Res., 112, C12013, doi:10.1029/2006JC003978, 2007.

Kwok, R., Cunningham, G., Wensnahan, M., Rigor, I., Zwally, H., and Yi, D.: Thinning and volume loss of the Arctic Ocean sea ice cover: 2003–2008, J. Geophys. Res., 114, C07005, doi:10.1029/2009JC005312, 2009.

Laxon, S., Peacock, N., and Smith, D.: High interannual variability of sea ice thickness in the Arctic region, Nature, 425, 947–950, doi:10.1038/nature02050, 2003.

Laxon, S. W., Giles, K. A., Ridout, A. L., Wingham, D. J., Willatt, R., Cullen, R., Kwok, R., Schweiger, A., Zhang, J., Haas, C., Hendricks, S., Krishfield, R., Kurtz, N., Farrell, S., and Davidson, M.: CryoSat-2 estimates of Arctic sea ice thickness and volume, Geophys. Res. Lett., 40, 732–737, doi:10.1002/grl.50193, 2013.

Lytle, V. and Ackley, S. F.: Snow-ice growth: a fresh water flux inhibiting deep convection in the Weddell Sea, Antarctica, Ann. Glaciol., 33, 45–50, doi:10.3189/172756401781818752, 2001.

Maaß, N., Kaleschke, L., Tian-Kunze, X., and Drusch, M.: Snow thickness retrieval over thick Arctic sea ice using SMOS satellite data, The Cryosphere, 7, 1971–1989, doi:10.5194/tc-7-1971-2013, 2013.

Markus, T. and Cavalieri, D. J.: Snow depth distribution over sea ice in the Southern Ocean from satellite passive microwave data, Antarct. Res. Ser., 74, 19–39, doi:10.1029/AR074p0019, 1998.

Markus, T. and Cavalieri, D. J.: An enhancement of the NASA Team sea ice algorithm, IEEE T. Geosci. Remote, 38, 1387–1398, 2000.

Markus, T. and Cavalieri, D. J.: AMSR-E Algorithm Theoretical Basis Document: Sea Ice Products, NASA, Greenbelt, MD, USA, 2008.

Markus, T., Cavalieri, D. J., Gasiewski, A. J., Klein, M., Maslanik, J. A., Powell, D. C., Stankov, B. B., Stroeve, J. C., and Sturm, M.: Microwave signatures of snow on sea ice: observations, IEEE T. Geosci. Remote, 44, 3081–3090, doi:10.1109/TGRS.2006.883134, 2006.

Maslanik, J. and Stroeve, J.: DMSP SSM/I-SSMIS Daily Polar Gridded Brightness Temperatures, version 4, October 2005–November 2007, NASA DAAC at the National Snow and Ice Data Center, Boulder, Colorado USA, 2004, updated 2012.

McPhee, M., Proshutinsky, A., Morison, J., Steele, M., and Alkire, M.: Rapid change in freshwater content of the Arctic Ocean, Geophys. Res. Lett., 36, L10602, doi:10.1029/2009GL037525, 2009.

Notz, D.: The future of ice sheets and sea ice: between reversible retreat and unstoppable loss, P. Natl. Acad. Sci. USA, 106, 20590–20595, doi:10.1073/pnas.0902356106, 2009.

Outten, S. and Esau, I.: A link between Arctic sea ice and recent cooling trends over Eurasia, Climatic Change, 110, 1069–1075, doi:10.1007/s10584-011-0334-z, 2012.

Parkinson, C. L., Cavalieri, D. J., Gloersen, P., Zwally, H. J., and Comiso, J. C.: Arctic sea ice extents, areas, and trends, 1978–1996, J. Geophys. Res., 104, 20837–20856, doi:10.1029/1999jc900082, 1999.

Pedersen, L. T.: Improved spatial resolution of SSM/I products, development of new satellite ice data products, Tech. rep., Nansen Environmental and Remote Sensing Center, Bergen, Norway, 1998.

Perovich, D., Jones, K., Light, B., Eicken, H., Markus, T., Stroeve, J., and Lindsay, R.: Solar partitioning in a changing Arctic sea-ice cover, Ann. Glaciol., 52, 192–196, doi:10.3189/172756411795931543, 2011.

Polyakov, I., Kwok, R., and Walsh, J.: Recent changes of arctic multiyear sea-ice coverage and the likely causes, B. Am. Meteorol. Soc., 93, 145–151, doi:10.1175/BAMS-D-11-00070.1, 2011.

Rampal, P., Weiss, J., and Marsan, D.: Positive trend in the mean speed and deformation rate of Arctic sea ice, 1979–2007, J. Geophys. Res., 114, C05013, doi:10.1029/2008JC005066, 2009.

Ramseier, R.: Sea Ice Validation, DMSP special sensor microwave/imager calibration/validation, Tech. Rep., Final Report Volume II, Naval Research Laboratory, Washington, DC, 1991.

Rothrock, D., Yu, Y., and Maykut, G.: Thinning of the Arctic sea-ice cover, Geophys. Res. Lett., 26, 3469–3472, 1999.

Schweiger, A., Lindsay, R., Zhang, J., Steele, M., Stern, H., and Kwok, R.: Uncertainty in modeled Arctic sea ice volume, J. Geophys. Res, 116, C00D06, doi:10.1029/2011JC007084, 2011.

Screen, J. and Simmonds, I.: The central role of diminishing sea ice in recent Arctic temperature amplification, Nature, 464, 1334–1337, doi:10.1038/nature09051, 2010.

Screen, J. A. and Simmonds, I.: Erroneous Arctic temperature trends in the ERA-40 reanalysis: a closer look, J. Climate, 24, 2620–2627, doi:10.1175/2010JCLI4054.1, 2011.

Screen, J. A. and Simmonds, I.: Declining summer snowfall in the Arctic: Causes, impacts and feedbacks, Clim. Dynam., 38, 2243–2256, doi:10.1007/s00382-011-1105-2, 2012.

Serreze, M. C., Maslanik, J. A., Key, J. R., Kokaly, R. F., and Robinson, D. A.: Diagnosis of the record minimum in Arctic sea ice area during 1990 and associated snow cover extremes, Geophys. Res. Lett., 22, 2183–2186, doi:10.1029/95GL02068, 1995.

Smedsrud, L. H., Sirevaag, A., Kloster, K., Sorteberg, A., and Sandven, S.: Recent wind driven high sea ice area export in the Fram Strait contributes to Arctic sea ice decline, The Cryosphere, 5, 821–829, doi:10.5194/tc-5-821-2011, 2011.

Smith, D. M. and Barrett, E. C.: Satellite mapping and monitoring of sea ice, unpublished final report to the Defence Research Agency, RSU, University of Bristol, 1994.

Spreen, G., Kern, S., Stammer, D., Forsberg, R., and Haarpaintner, J.: Satellite-based estimates of sea-ice volume flux through Fram Strait, Ann. Glaciol., 44, 321–328, doi:10.3189/172756406781811385, 2006.

Stroeve, J., Serreze, M., Holland, M., Kay, J., Malanik, J., and Barrett, A.: The Arctic's rapidly shrinking sea ice cover: a research synthesis, Climatic Change, 110, 1005–1027, doi:10.1007/s10584-011-0101-1, 2012.

Svendsen, E., Kloster, K., Farrelly, B., Johannessen, O., Johannessen, J., Campbell, W., Gloersen, P., Cavalieri, D., and Mätzler, C.: Norwegian remote sensing experiment: Evaluation of the Nimbus 7 scanning multichannel microwave radiometer for sea ice research, J. Geophys. Res., 88, 2781–2791, doi:10.1029/JC088iC05p02781, 1983.

Svendsen, E., Matzler, C., and Grenfell, T.: A model for retrieving total sea ice concentration from a spaceborne dual-polarized passive microwave instrument operating near 90 GHz, Int. J. Remote Sens., 8, 1479–1487, 1987.

Swift, C., Fedor, L., and Ramseier, R.: An algorithm to measure sea ice concentration with microwave radiometers, J. Geophys. Res., 90, 1087–1099, 1985.

Tietsche, S., Notz, D., Jungclaus, J., and Marotzke, J.: Recovery mechanisms of Arctic summer sea ice, Geophys. Res. Lett., 38, L02707, doi:10.1029/2010GL045698, 2011.

Timco, G. and Frederking, R.: A review of sea ice density, Cold Reg. Sci. Technol., 24, 1–6, 1996.

Tonboe, R. T., Pedersen, L. T., and Haas, C.: Simulation of the CryoSat-2 satellite radar altimeter sea ice thickness retrieval uncertainty, Can. J. Remote Sens., 36, 55–67, 2010.

Warren, S., Rigor, I., Untersteiner, N., Radionov, V., Bryazgin, N., Aleksandrov, Y., and Colony, R.: Snow depth on Arctic sea ice, J. Climate, 12, 1814–1829, doi:10.1175/1520-0442(1999)012<1814:SDOASI>2.0.CO;2, 1999.

Willat, R., Laxon, S., Giles, K., Cullen, R., Haas, C., and Helm, V.: Ku-band radar penetration into snow cover on Arctic sea ice using airborne data, Ann. Glaciol., 52, 197–205, doi:10.3189/172756411795931589, 2011.

Yi, D. and Zwally, J.: Arctic Sea Ice Freeboard and Thickness, National Snow and Ice Data Center, Boulder, Colorado, USA, available at: http://nsidc.org/data/docs/daac/nsidc0393_arctic_seaice_freeboard/index.html, (last access: 31 March 2013) 2009.

Zwally, H. J., Schutz, B., Abdalati, W., Abshire, J., Bentley, C., Brenner, A., Bufton, J., Dezio, J., Hancock, D., Harding, D., Herring, T., Minster, B., Quinn, K., Palm, S., Spinhirne, J., and Thomas, R.: ICESat's laser measurements of polar ice, atmosphere, ocean, and land, J. Geodyn., 34, 405–445, doi:10.1016/S0264-3707(02)00042-X, 2002.